REPORT DOCUMENTATION PAGE

Form Approved OMB No. 0704-0188

1. REPORT DATE *(DD-MM-YYYY)*	2. REPORT TYPE	3. DATES COVERED *(From – To)*
06-07-2010	Final Report	28 August 2009 - 28-Jul-10

4. TITLE AND SUBTITLE

Verification of parallel C code for specific absorption rate (SAR) of electromagnetic fields (EMF)

5a. CONTRACT NUMBER
FA8655-09-1-3045

5b. GRANT NUMBER

5c. PROGRAM ELEMENT NUMBER

6. AUTHOR(S)

Professor PETER GAJSEK

5d. PROJECT NUMBER

5d. TASK NUMBER

5e. WORK UNIT NUMBER

7. PERFORMING ORGANIZATION NAME(S) AND ADDRESS(ES)
Institute of non-ionizing radiation
Pohorskega bataljona 215
Ljubljana 1000
Slovenia

8. PERFORMING ORGANIZATION REPORT NUMBER
N/A

9. SPONSORING/MONITORING AGENCY NAME(S) AND ADDRESS(ES)

EOARD
Unit 4515 BOX 14
APO AE 09421

10. SPONSOR/MONITOR'S ACRONYM(S)

11. SPONSOR/MONITOR'S REPORT NUMBER(S)
Grant 09-3045

12. DISTRIBUTION/AVAILABILITY STATEMENT: Approved for public release; distribution is unlimited. (approval given by local Public Affairs Office)

13. SUPPLEMENTARY NOTES

14. ABSTRACT This report results from a contract tasking Institute of non-ionizing radiation as follows: The main part of the proposed work will be designed to verify the parallel C code with the published results obtained by the Fortran code. To carry out trustful verification of the parallel FDTD code, it is necessary to compare the result of the parallel C code with the results of the Fortran code for different exposure conditions and different anatomical models. In the first step, it is necessary to decide which models will be included in the calculations ad for which exposures the calculation will be run. At least two different anatomical models will be included in the calculation: human and rat. The calculations will cover the most investigated frequencies in the frequency spectrum 80-3000 MHz as well as some selected frequencies at the upper and lower end of the code capability. In the verification, all important areas of program package will be included: automatic space partitioning algorithm, importing of the tissue data, model data and boundary data, clustering. Beside the verification of the parallel C code also comparison of the time effectiveness of both codes will be prepared.
The results show great consistency between the two different implementations of FDTD code across a wide variety of models and exposure scenarios. There are some minor outliers in the whole body SAR comparison, and some larger differences in the localized tissue SAR values. However, these can be explained by the fact that although the model and exposure details were the same, the criteria for finishing a simulation (i.e. the ratio between two successive whole-body SAR values) can be satisfied over the whole body, even if the distribution of power over the internal organs is not entirely stabilized yet. The values would converge better if much longer simulations (in terms of number of halfcycles of the incident field, or number of time-steps of the Yee algorithm) were used. However, when tissue SAR values are much lower than the basic restrictions on localized SAR, the discrepancies in the range of 30 % are not significant. In fact, the best measurement setups for measuring localized SAR values in homogeneous liquid-filled phantoms have a measurement uncertainty around 1 dB (around 20 %), so differences in localized tissue values in this range actually represent a very good result. The comparison with third party software SEMCAD also showed, that the results are very good and especially whole-body SAR values agreed very well, considering the differences in voxeling, normalization and most importantly SAR statistics algorithms.Although some values show rather large differences, this could also be in part due to different hardware setups that the results were obtained on or due to different approaches to parallelization. The conclusion is, that the two different implementations of the FDTD algorithm produce very similar results, to the point of being indistinguishable.

15. SUBJECT TERMS
EOARD, Modeling & Simulation, Electromagnetic Fields

16. SECURITY CLASSIFICATION OF:			17. LIMITATION OF ABSTRACT	18, NUMBER OF PAGES	19a. NAME OF RESPONSIBLE PERSON
a. REPORT	b. ABSTRACT	c. THIS PAGE			TAMMY SAVOIE, Lt Col, USAF
UNCLAS	UNCLAS	UNCLAS	UL	32	19b. TELEPHONE NUMBER *(Include area code)* +44 (0)1895 616459

INSTITUTE OF NON-IONIZING RADIATION

INŠTITUT ZA NEIONIZIRNA SEVANJA

RESEARCH PROJECT:

Award No.: FA 8655-09-1-3045

Verification of the parallel C code with Fortran code for FDTD calculations

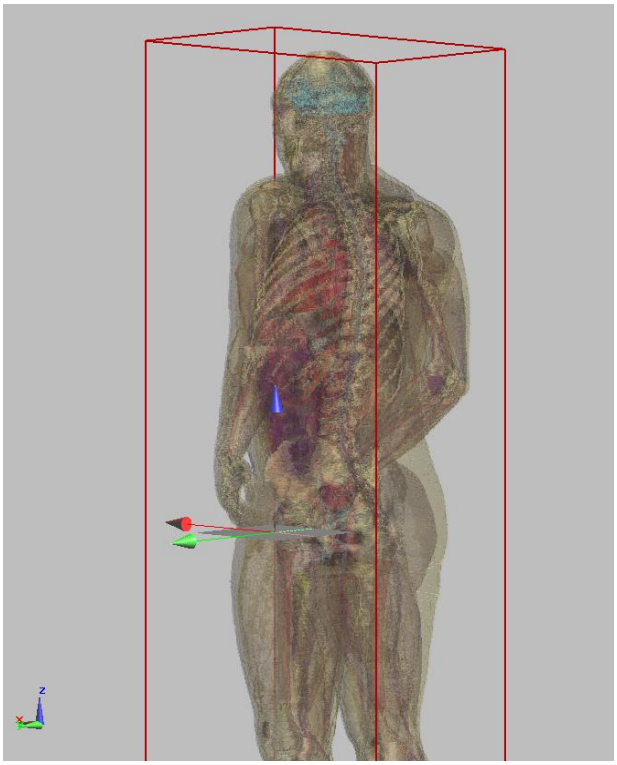

FINAL REPORT

Ljubljana, 4.7.2010

INŠTITUT ZA NEIONIZIRNA SEVANJA

dr.Peter Gajšek

Table of Contents

1. Introduction

The health and safety electromagnetic fields (EMF) standards in the radio frequency (RF) range are primarily based on the concept of a thermal mechanism and protect against “thermal” effects. Indeed, the current consensus is that only thermal RF effects could be harmful, but this certainly does not mean that studies reporting possible non-thermal effects were ignored. This consensus is based on rigorous analysis of published studies, which have to satisfy such strict criteria as replication in several species, under different field conditions, and that the effects could be considered potentially harmful in humans. A brief review of some RF safety standards, such as the International Commission of Non-ionizing Radiation Protection (ICNIRP) and Institute of Electrical and Electronics Engineers, Inc. (IEEE) standards (ICNIRP 2009; IEEE 2006), reveals that they include consideration of frequency dependent absorption in human body (whole body resonance). In addition, special restrictions on localized exposure including methods for volume averaging are introduced. These documents specify time-averaged whole-body-averaged SAR values and peak spatial-average SAR values, neither of which should be exceeded. The spatial peak SAR is usually averaged over a specified volume of 10 grams (contiguous tissue (ICNIRP 2009)). Current RF exposure standards are generally derived from an assumption of uniform field exposure of the entire body. While the fundamental basis of these standards is related to limiting the SAR in the body, as averaged over the entire body mass, most standards, such as those of the (IEEE 2006) and (ICNIRP 2009), also contain Maximum Permissible Exposure (MPE) limits and reference levels related to peak SAR that may occur at any point within the body, averaged over 10 grams of tissue. These spatial peak SAR limits are derived from observations of uniform exposure of laboratory animals or phantom models of both animals and humans. In recognition of the non-uniform absorption of RF energy within the body, even with uniform field exposure over the body, the standards set a limit on the spatial peak SAR at 25 times the whole-body average value. For example, while the whole-body average SAR is limited to 0.4 watts per kilogram (W/kg) in the whole body, a local SAR of 10 W/kg, averaged over 10 grams of tissue, is permitted. For determining SAR values inside the human body, two approaches have been established. The first is measurement in body-simulating liquid filled phantoms, while the second is numerical dosimetry. For measurements, the liquid represents a homogeneous body with a constant conductivity and relative permittivity. Numerical simulations can on the other hand provide the possibility of investigating exposure of specific organs with more realistic tissue and geometric properties.

There are several methods for simulating the interaction of electromagnetic fields with the body, based on different numerical approaches (Hand 2008); finite-difference time-domain, in short FDTD is among the most commonly used for dosimetric applications, due to its robustness, relative simplicity of implementation and favorable scaling of computing cost versus problem size. FDTD is a numerical method for solving full-wave Maxwell equations in settings with complex geometries and/or incident electromagnetic fields (Talfove and Hagness 2005). The method was pioneered by Yee in 1966, who devised an algorithm where the *E* and *H* fields are computed in separate steps using second-order finite difference approximation of the Maxwell equations (Yee 1966). The FDTD algorithm lends itself to very efficient parallelization, thus enabling the use of supercomputers, cluster computing and recently also parallel computing on graphics processing units (Inman and Elsherbeni 2005).

The main objective of this project is to verify the parallel C code program package for FDTD calculations of human exposure due to the electromagnetic fields (EMF) which was developed by Radio Frequency Radiation Branch, AFRL, Brooks City-Base, Texas with parallel Fortran code which gained wide confidence in the results among the scientists (Gajsek et al. 2002; Gajsek et al. 2001). The older algorithm written in Fortran and based on LAM/MPI clustering and message parsing platform in Linux was used as a benchmark for verification. The second implementation is written in C and runs on OpenMPI clustering platform, also in Linux. Both platforms were also compared with third-party commercial FDTD software package SEMCAD X (Speag, Zurich, Switzerland).

With this effort AFRL and INIS could fully compare the existing methods and equipment for SAR predictions in various digital numerical models and, thus, increase the confidence in numerical dosimetry results. An error margin will be analyzed and fully described that is due to computer hardware and software tools and different programming language.

2. Protocol definition

To provide a framework for the verification, a protocol was defined, before the verification was performed. The protocol was defined in order to provide a framework for comparing the two different versions of FDTD code. A range of different models and exposure scenarios was chosen to represent typical uses of the software. The models chosen for the comparison were the 1mm man (1878 by 340 by 584 voxels), the 2mm man (939 by 179 by 293 voxels), the 3mm man (196 by 114 by 626 voxels) and a rat model (51 by 22 by 114 voxels).

A computer-segmented set of the photographic images was created by National University of Singapore and Johns Hopkins University. Each of the 1878 slices in the XY plane was then more segmented with a palette of colors that represented the 40 tissue types (the method of construction is described in (PA Mason et al. 1995)). Each voxel is a cube 1 mm on a side and the model consists of 374 million voxels (1878 x 340 x 586 voxels). Predicting SAR values in this 1 mm^3 whole-body model using FDTD requires a minimum of 18 GB of computer memory. Since this high-resolution model requires a substantial amount of computer memory, smaller versions of this dataset have been created and are suitable for some applications.

These reduced resolution (2 mm and 3 mm) models were created automatically. The process was as follows for creating a 3-mm anatomical model from a 1-mm model. Layers of air were added to one or more sides of the model volume to make the size of the model an even multiple of the 3 mm^3. The reduction then takes a cube of 3 by 3 by 3 one-millimeter voxels and based on the most common type in that cube creates the single 3 mm voxel. This process was repeated for each 3 by 3 by 3 set of 1-mm voxels.

The models were used to calculate the SAR distribution in a planewave exposure in two different incident field orientations, MEHK (θ=90°, ϕ=270°, $E_{inc\theta}$=1, $E_{inc\phi}$=0, E_{Peak}=1 V/m) and PEHK (θ=90°, ϕ=90°, $E_{inc\theta}$=1, $E_{inc\phi}$=0, E_{Peak}=1 V/m), within a frequency range from 70 to 2000 MHz. The criteria for comparison were the maximum tissue SAR for all tissues, the whole body SAR for each model and frequency and SAR in the vertical plane through the centre of the model. The difference in each data point should be less than ± 10 %.

FDTD code is well known and widespread numerical modeling technique to calculate field distribution inside the human exposed to electromagnetic field. In Brooks AFRL the code was developed about 10 years ago and lately intensively used in the filed of numerical dosimetry. The original code, which is freely available, is written in Fortran. It was used as a base for some of the commercially available program packages for FDTD calculation.

Since in the last few years C programming language is becoming more popular than the Fortran the FDTD code was rewritten in the C. The old Fortran FDTD code was widely accepted and used as a suitable method for numerical calculations of electromagnetic field exposures. Before a wide use of the new C code verification is needed for this code. Verification is a process which requires parametric analysis and calculations of SAR values for different voxel models. By comparing the results of a set of calculations with the Fortran code with the same set of calculations with the C code we will validate the C code. It is important to plane the set of the calculations to minimize the possibility to overlook errors or faults in the C code.

Additionally the evaluation of the effect of number of PML and air layers on the SAR values was investigated, and the speed and parallel efficiency of calculation were compared between the two implementations of the FDTD algorithm, as well as a comparison with the third-party SEMCAD X software.

For the calculations a cluster of multi processor computers is used. It consists of two multi processor computers, in each computer 2 quad core Xeon processors at 1.6 GHz and 12 GB RAM is installed, altogether 16 cores and 24 GB of RAM is available.

There is Centos 5 installed on the computers as well as the intel Fortran 9 compiler and LAM-MPI. On the cluster, parallel Fortran version of Brooks FDTD code is running.

3. Results

1 mm man model

This was the highest resolution and the largest model used in the calculation. The result was performed at only one frequency – 2000 MHz, with the problem size being approximately 447 Mcells. The incident field orientation was MEHK (θ=90°, ϕ=270°, $E_{inc\theta}$=1, $E_{inc\phi}$=0, E_{Peak}=1 V/m). The total computation time was 48 hours and 50 minutes, the number of time-steps in the simulation was 2080. This gives an average calculation speed of 5.3 Mcells/second.

The results of the 1mm model show a 9 % difference in results between the C and Fortran codes for the whole body SAR, as shown in Table 1.

Frequency [MHz]	Fortran [W/kg]	C [W/kg]	% difference
100	0.051812	0.047322	-9 %

Table 1: Results of the 1mm model in the Fortran and C codes

The mean normalized difference of the maximum tissue SAR values (shown in Table 2) is -29 %, while the mean normalized difference of the mean tissue SAR is -25 %. If the values for the normalized difference are weighted with the number of voxels in each tissue, the values are -0.5 % and -0.2 % for maximum and mean tissue SAR, respectively. Tissue SAR values correspond in all mentioned cases to the maximum (single voxel) SAR in the tissue, or the mean tissue SAR, i.e. the average of SAR values over all voxels in the tissue.

tissue	C code		Fortran code	
	max sar [W/kg]	mean sar [W/kg]	max sar [W/kg]	mean sar [W/kg]
BILE	0.006099	0.001566	0.21235	0.041979
BODY FLUID	0.993493	0.012824	2.9976	0.046456
EYE (cornea)	0.042668	0.013682	0.93334	0.29773
FAT	3.89667	0.021974	10.484	0.020427
LYMPH	0.416686	0.001601	1.8877	0.021414
MUSCOUS MEMBRANE	0.352977	0.003615	4.361	0.055832
NAILS (toe & finger)	0.817338	0.077769	1.7624	0.20442
NERVE (spine)	2.548601	0.027095	0.74659	0.014396
MUSCLE	8.617774	0.049307	6.5786	0.048736
HEART	0.01187	0.001232	0.12807	0.005391
WHITE MATTER	0.323376	0.026388	0.19767	0.016669
STOMACH	0.023238	0.001423	0.76467	0.012716
GLANDS	1.002455	0.010366	1.6377	0.077203
BLOOD VESSEL	5.64557	0.038411	8.5819	0.076469
LIVER	0.141912	0.002211	0.3282	0.005453
GALL BLADDER	0.008603	0.001348	0.43787	0.025449
SPLEEN	0.113244	0.005189	0.048623	0.001684
CEREBELLUM	0.162809	0.018788	0.038388	0.002358
BONE (cortical)	1.168127	0.011145	2.358	0.027413
CARTILAGE	2.85327	0.015508	10.071	0.081094
LIGAMENTS	3.761534	0.053455	5.8432	0.10828
SKIN/DERMIS	10.53239	0.298725	39.166	0.3207
INTESTINE (large)	0.479863	0.003542	1.0679	0.026054
TOOTH	0.008644	0.000684	0.4391	0.029196
GRAY MATTER	0.421018	0.034685	0.61099	0.02381
EYE (lens)	0.029349	0.008608	0.85487	0.27268
LUNG (outer)	0.094155	0.003409	0.25997	0.011928
INTESTINE (small)	0.066383	0.00205	1.1012	0.019203
EYE (sclera/wall)	0.084886	0.010594	2.0483	0.21677
LUNG (inner)	0.253398	0.00549	1.014	0.014397
PANCREAS	0.010921	0.001199	0.006803	0.001053
BLOOD	7.328976	0.013444	7.0858	0.037708
CEREBRAL SPINAL FLUI	0.692121	0.053989	0.80209	0.035709
EYE (aqueous humor)	0.071214	0.019881	1.1122	0.33588
KIDNEYS	0.02343	0.001701	0.007199	0.001126
BONE MARROW	0.534079	0.007642	1.4257	0.015365
BLADDER	0.014046	0.000656	3.1387	0.01044
TESTICLES	0.003193	0.001209	1.1866	0.25478
BONE (cancellous)	1.391796	0.017978	1.8113	0.032798

Table 2: Tissue maximum and mean SAR in the 1mm man model.

2 mm man model

The 2 mm man was run in a frequency range from 100 to 2000 MHz, with a step of 100 MHz, in the MEHK (θ=90°, ϕ=270°, $E_{inc\theta}$=1, $E_{inc\phi}$=0, E_{Peak}=1 V/m) incident field orientation. The values of whole-body SAR are presented in Table 3.

Frequency [MHz]	Fortran [W/kg]	C [W/kg]	% difference
100	0.113036	0.111546	-1%
200	0.053451	0.069123	29%
300	0.056834	0.057689	2%
400	0.063927	0.06077	-5%
500	0.065186	0.061973	-5%
600	0.065161	0.062287	-4%
700	0.063500	0.061336	-3%
800	0.063326	0.060706	-4%
900	0.062653	0.060285	-4%
1000	0.062618	0.061052	-3%
1100	0.061655	0.059845	-3%
1200	0.061946	0.059239	-4%
1300	0.062763	0.059063	-6%
1400	0.062146	0.058634	-6%
1500	0.060409	0.058475	-3%
1600	0.058856	0.057524	-2%
1700	0.057357	0.056685	-1%
1800	0.056709	0.055575	-2%
1900	0.055952	0.054456	-3%
2000	0.055794	0.053205	-5%

Table 3: Whole-body SAR values for the 2mm man model

The values of whole-body SAR versus frequency are plotted in Figure 1. In all the data points but one, the whole-body SAR from the two different versions of the code does not differ by more than 6 %, with the Fortran code generally producing slightly higher values than the C code. A statistical analysis was performed on the two sets of data to compare the results of the two different codes. The difference between each case at every frequency was compared to determine if there was any statistically significant difference between the results. In each case, a **Wilcoxon signed rank test** was used, since the results were not distributed normally (**Shapiro-Wilk** test for normality ($P < 0.050$)). The non-normality of the distribution of results prevented the use of a paired t-test. The results of the analysis show, that for the 2 mm man, there is a significant difference between the two different codes (P=0.001).

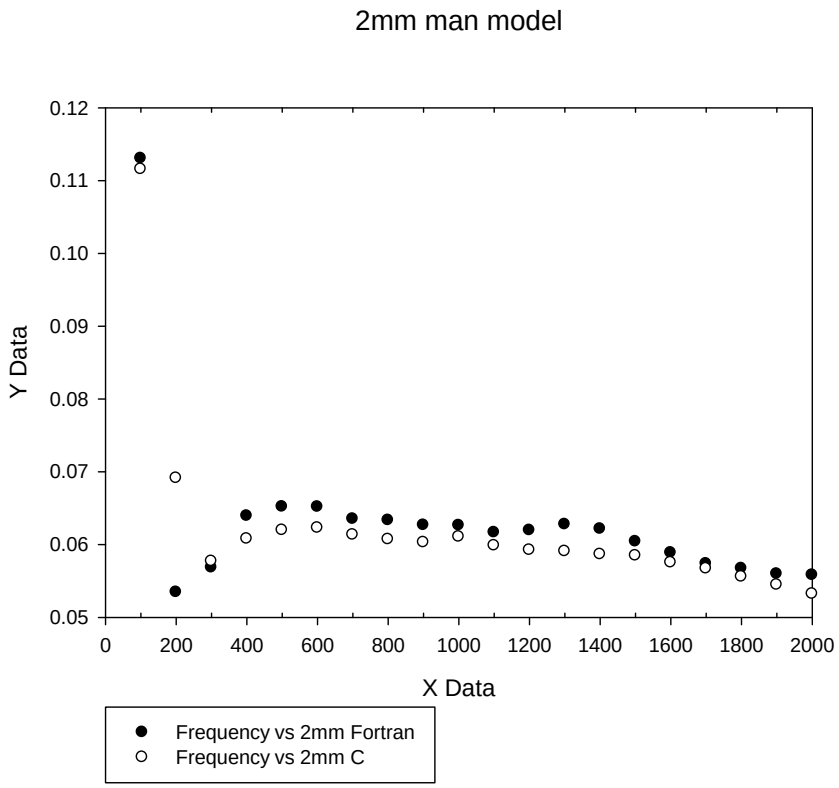

Figure 1: Whole body SAR in 2mm man model vs. frequency.

Tissue/organ maximum and mean SAR values were also compared. The largest differences for maximum SAR were 252 % (all percentages were calculated with the formula $(SAR_C\text{-}SAR_F)/SAR_F$) in the tissue “stomach” at 100 MHz, and -75 % in the tissue “kidneys” at 1600 MHz. The average error was 8 %, with the standard deviation of the error being 35 %. These values are much smaller for mean tissue SAR, which is expected, since these are representative of the whole tissue mass, which can range from a less than a gramm to several kilograms (from 42 cells, or less than a gramm for tissue “bile”, to more than 5 million cells and more than 40 kilograms for tissue “muscle”). The maximum difference in the mean tissue SAR were 81 % in the tissue “lymph” at 200 MHz, and -55% in the tissue “spleen” at 1200 MHz. The mean difference was 1 % while the standard deviation was 15 %.

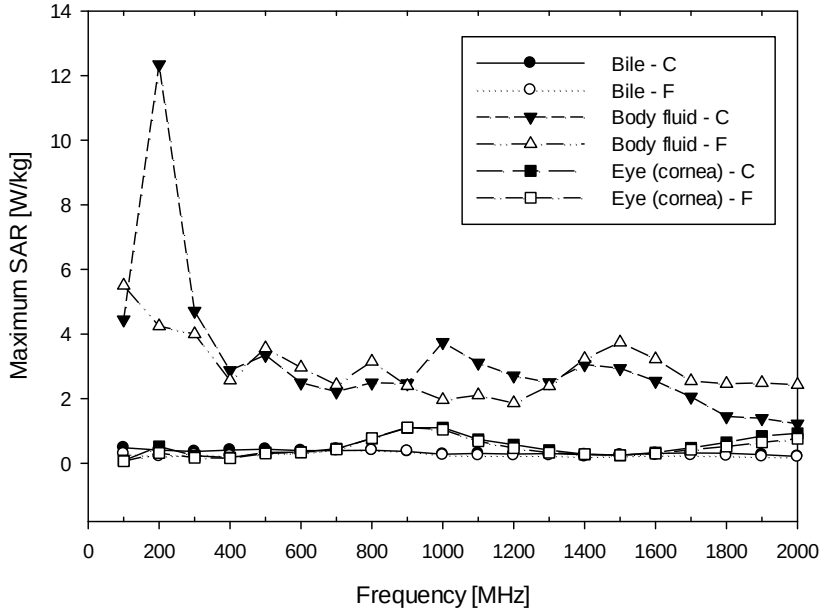

Figure 2: Maximum tissue SAR values for tissues "bile", "body fluid" and "eye – cornea"

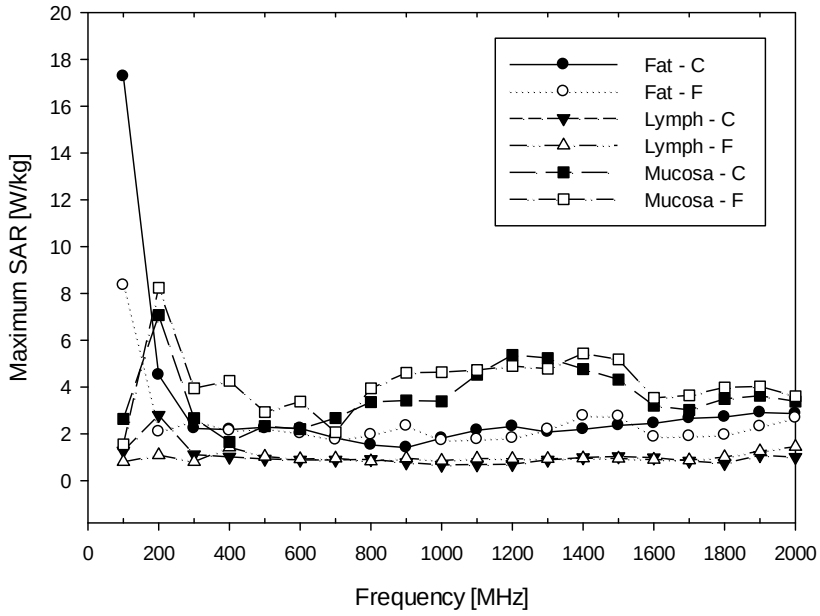

Figure 3: Maximum tissue SAR values for tissues "fat", "lymph" and "mucous membrane"

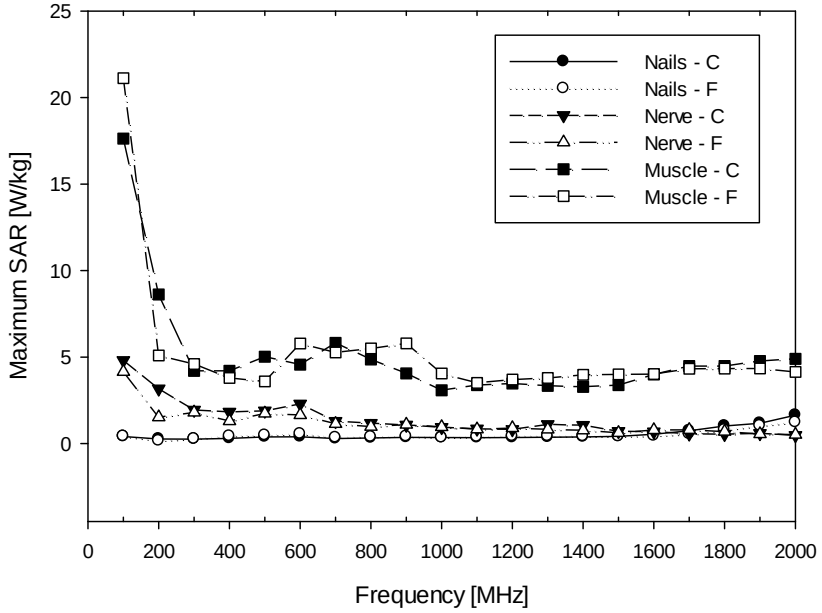

Figure 4: Maximum tissue SAR values for tissues "nails", "nerve" and "muscle"

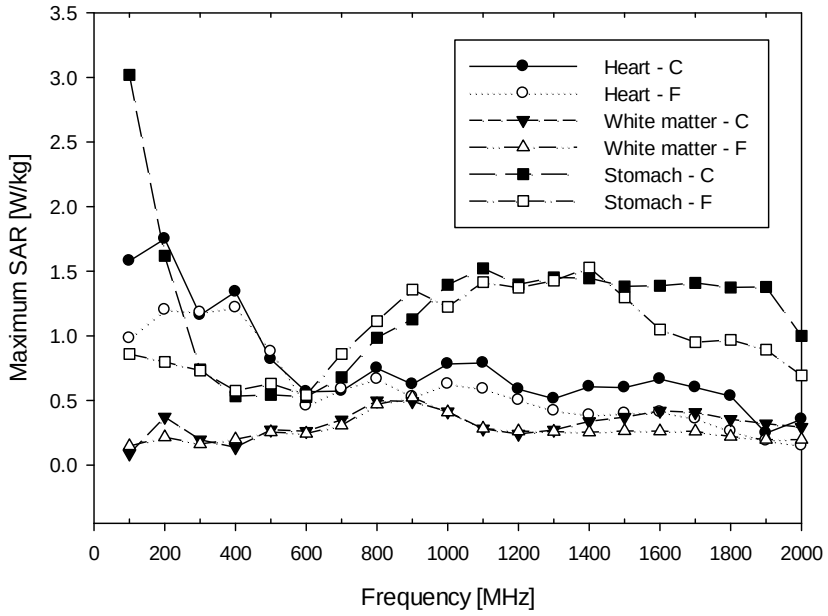

Figure 5: Maximum tissue SAR values for tissues "heart", "white matter" and "stomach"

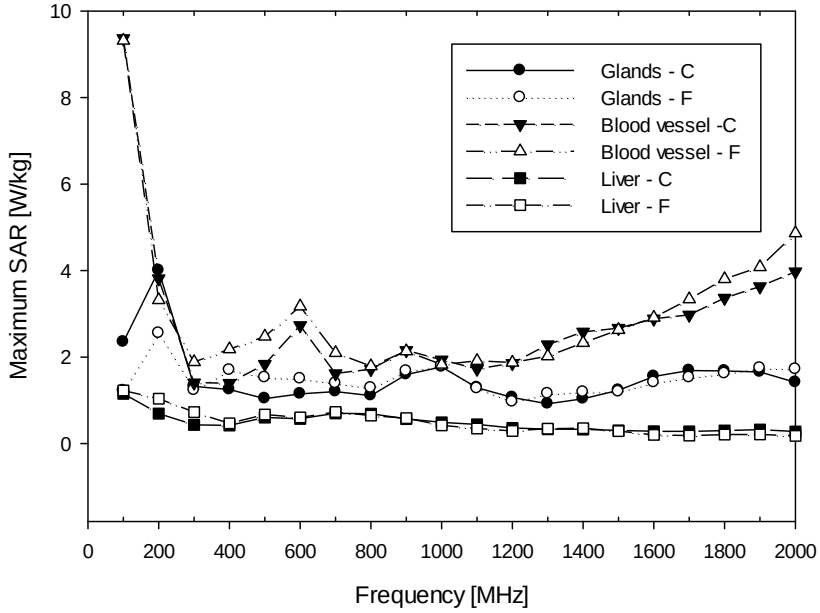

Figure 6: Maximum tissue SAR values for tissues "glands", "blood vessel" and "liver"

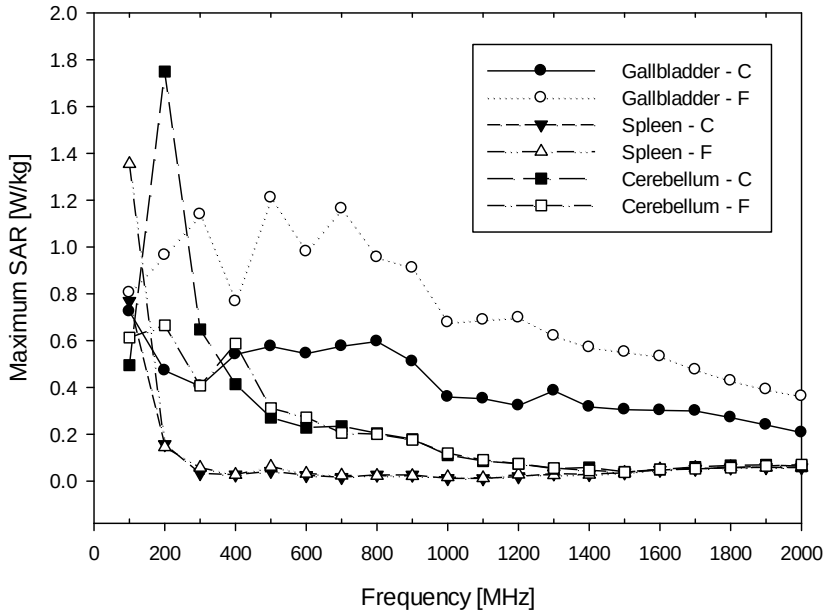

Figure 7: Maximum tissue SAR values for tissues "gallbladder", "spleen" and "cerebellum"

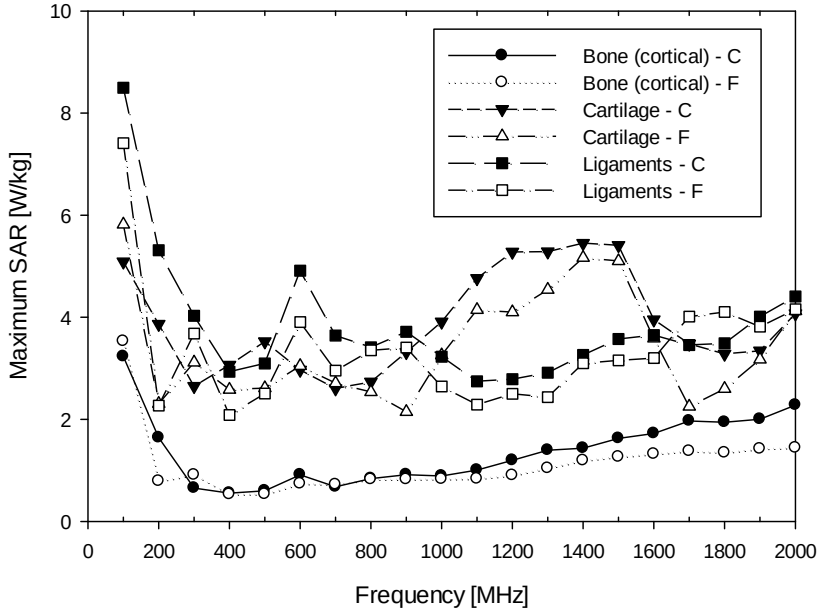

Figure 8: Maximum tissue SAR values for tissues "bone - cortical", "cartilage" and "ligaments"

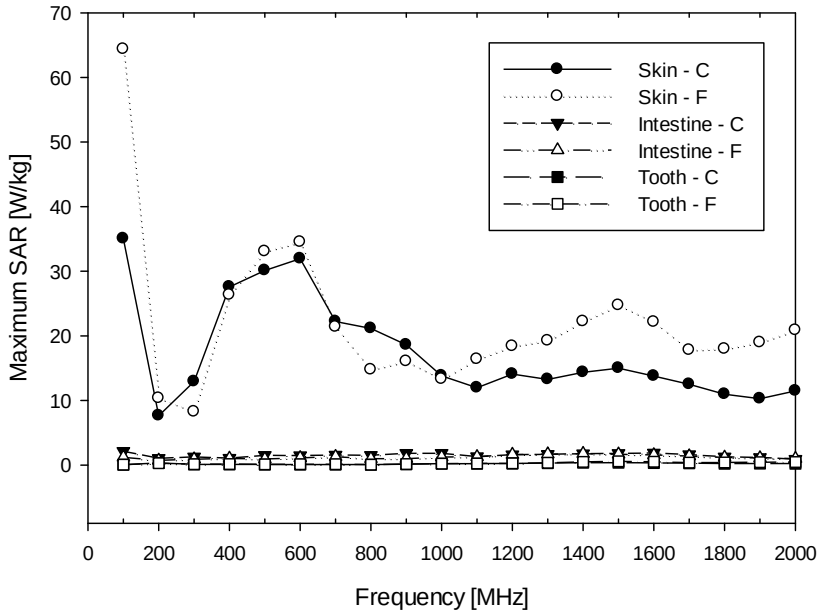

Figure 9: Maximum tissue SAR values for tissues "skin", "intestine" and "tooth"

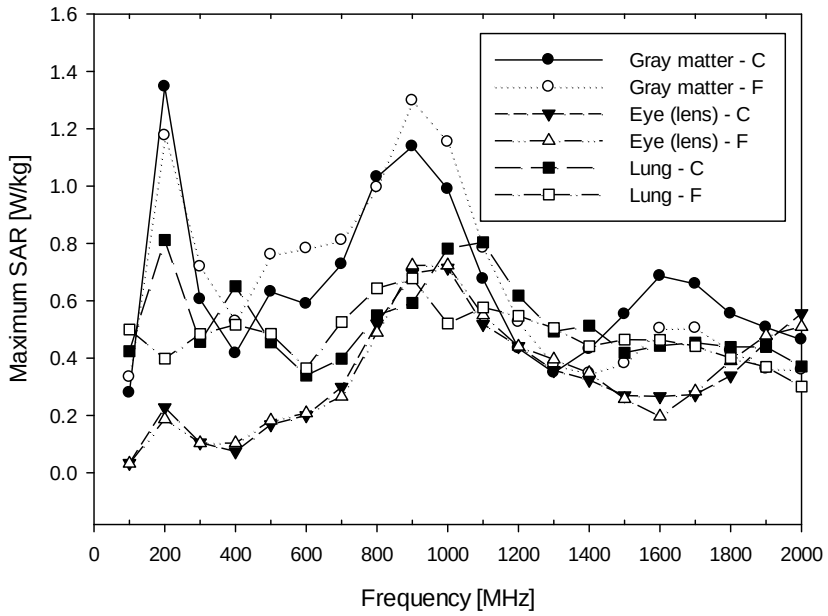

Figure 10: Maximum tissue SAR values for tissues "gray matter", "eye - lens" and "lung"

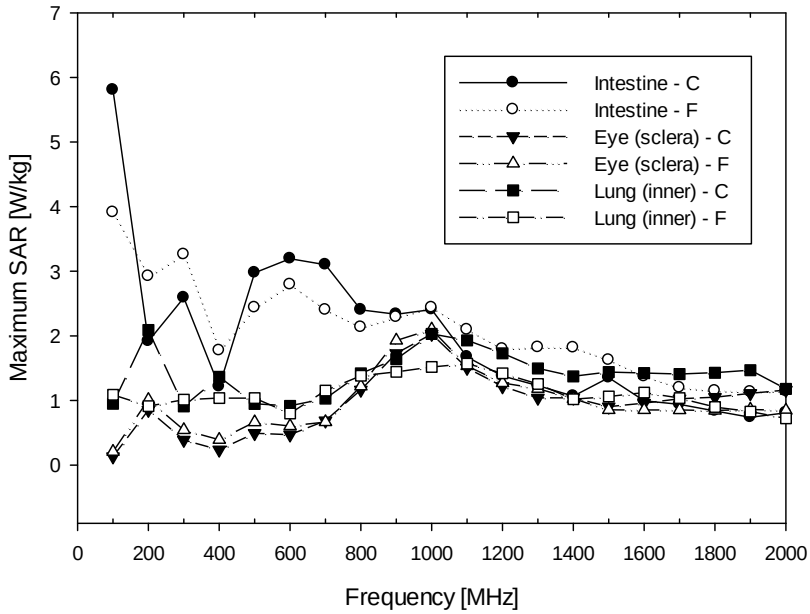

Figure 11: Maximum tissue SAR values for tissues "intestine", "eye - sclera" and "lung - inner"

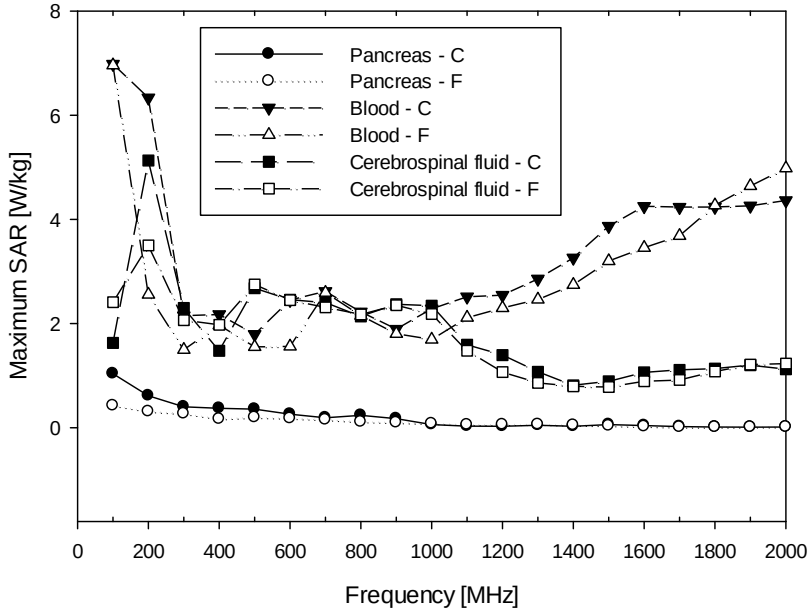

Figure 12: Maximum tissue SAR values for tissues "pancreas", "blood" and "cerebrospinal fluid"

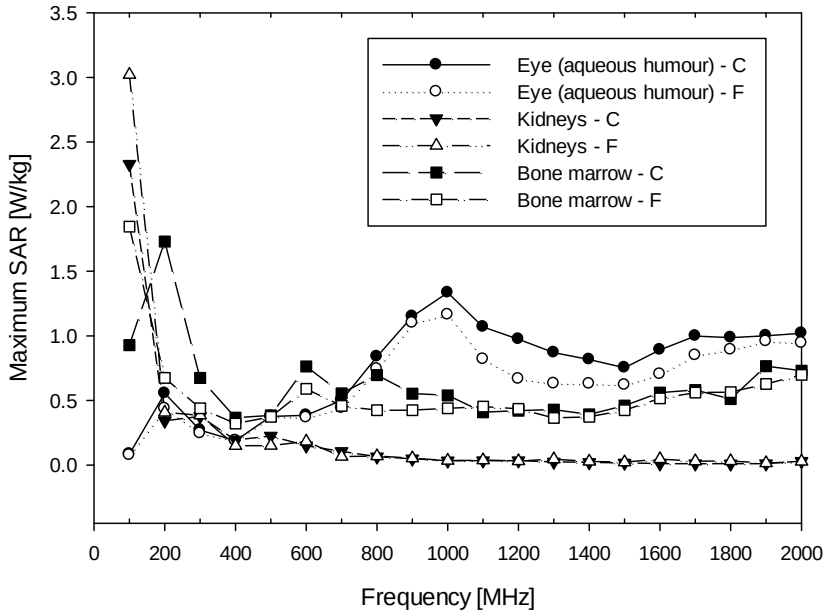

Figure 13: Maximum tissue SAR values for tissues "eye – aqueous humor", "kidneys" and "bone marrow"

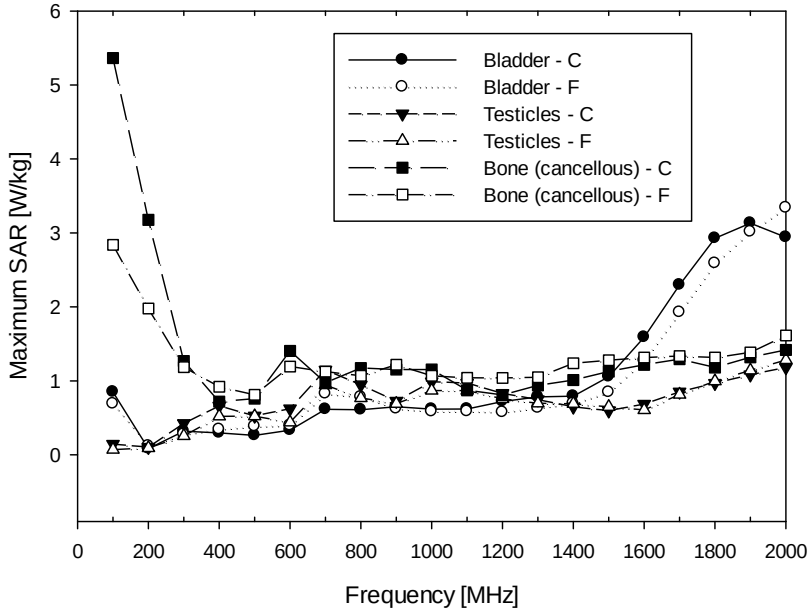

Figure 14: Maximum tissue SAR values for tissues "bladder", "testicles" and "bone - cancellous"

Figures 2-14 above show the frequency dependency of each different tissue type as calculated by the two different FDTD implementations. The graphs show a good agreement in tissue SAR values across a very broad range of frequencies and different tissue permittivities and conductivities.

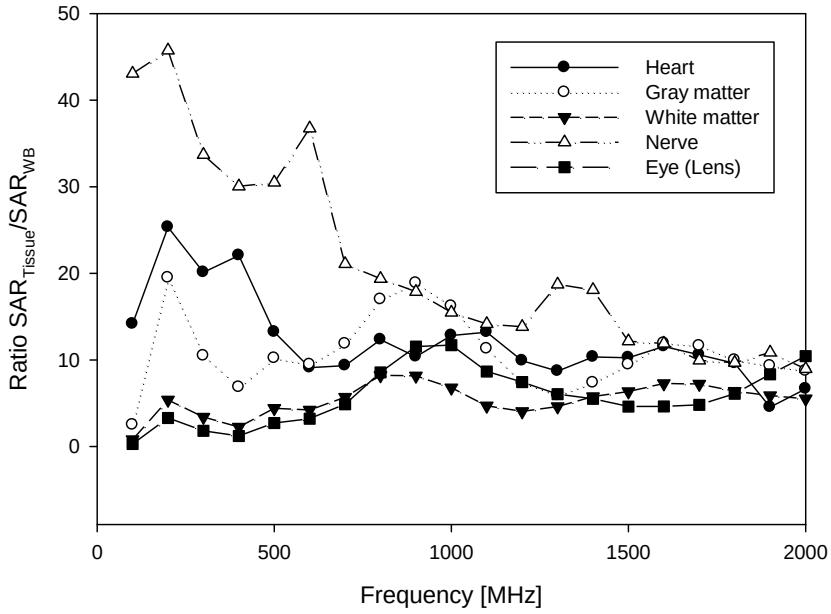

Figure 15: Ratio between maximum tissue SAR and whole-body SAR

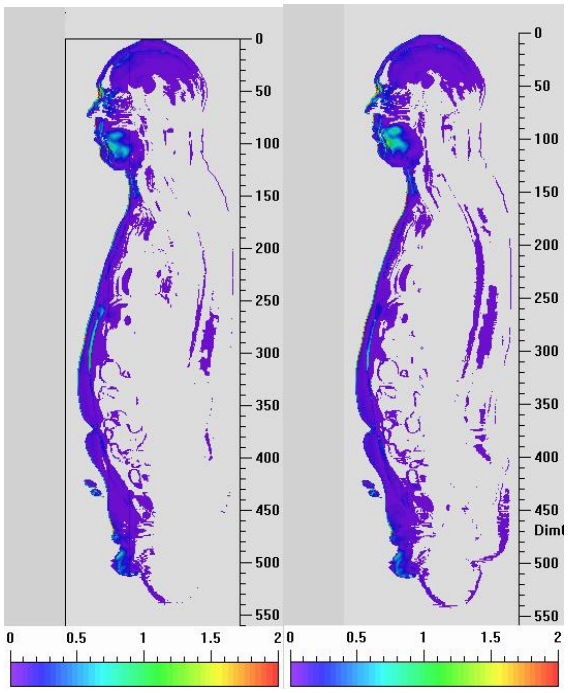

Figure 16: SAR in the middle of the body in the 2 mm man. Left: result of C code. Right: result of Fortran code.

The ratio of tissue maximum SAR / whole-body SAR versus frequency is shown in Figure 15. Although the use of tissue maximum SAR instead of an average over 10 g of tissue was used, which yields a significantly more conservative results, the maximum SAR / whole-body SAR ratio is lower than the 25 recommended by the international guidelines and standards in all investigated tissues (Heart, Grey matter, White matter, Eye lens and Nerve), at frequencies above 800 MHz. It is higher than 25 only in the tissue Nerve at lower frequencies which may be the result of a few single voxels with very high values of SAR.

3 mm man model

The two codes were compared in a total of 20 points, of which 10 were in the MEHK (θ=90°, ϕ=270°, $E_{inc\theta}$=1, $E_{inc\phi}$=0, E_{Peak}=1 V/m) and 10 in the PEHK (θ=90°, ϕ=90°, $E_{inc\theta}$=1, $E_{inc\phi}$=0, E_{Peak}=1 V/m) incident field configuration.

Field orientation	Frequency [MHz]	Fortran [W/kg]	C [W/kg]	% difference
MEHK	200	0.05352	0.06938	30%
	400	0.06362	0.06122	-4%
	600	0.06498	0.06243	-4%
	800	0.0633	0.06106	-4%
	1000	0.06243	0.06163	-1%
	1200	0.06087	0.0604	-1%
	1400	0.06125	0.06121	0%
	1600	0.06035	0.06041	0%
	1800	0.0588	0.05908	0%
	2000	0.05737	0.05732	0%
PEHK	200	0.04888	0.06447	32%
	400	0.06158	0.05899	-4%
	600	0.06702	0.06357	-5%
	800	0.06437	0.06312	-2%
	1000	0.06347	0.06313	-1%
	1200	0.06176	0.06147	0%
	1400	0.06053	0.06071	0%
	1600	0.05842	0.05855	0%
	1800	0.05684	0.05656	0%
	2000	0.05542	0.05548	0%

Table 4: Whole body SAR results for the 3 mm man model

The results are presented in Table 4. All results above 200 MHz show very good agreement between the two different codes, while the frequencies below show slightly larger errors. The largest difference of 32 % was found at 200 MHz. The values of whole-body SAR versus frequency are shown also in Figure 17 below.

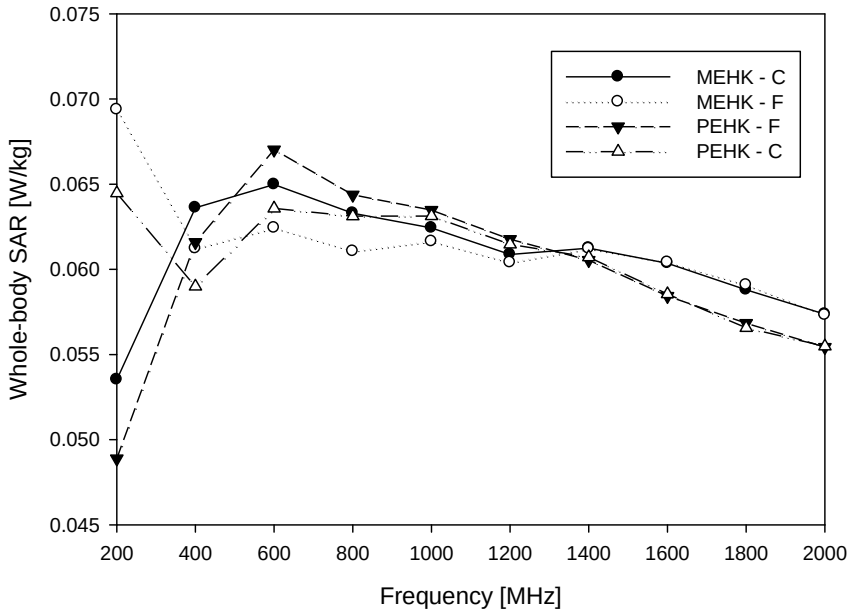

Figure 17: Whole body SAR in 3mm man model vs. frequency

4. The role of boundary conditions

A statistical analysis was performed on the two sets of data to compare the results of the two different codes. The difference between each case at every frequency was compared to determine if there was any statistically significant difference between the results. In each case, a **Wilcoxon signed rank test** was used, since the results were not distributed normally (**Shapiro-Wilk** test for normality ($P < 0.050$)). The non-normality of the distribution of results prevented the use of a paired t-test. The results of the analysis show, that for the 3mm model, no significant difference was observed in the results ($P=1$).

The 3 mm model was also used to evaluate the effect of varying the number of air layers and PML layers. The results are shown in Figures 18 and 19.

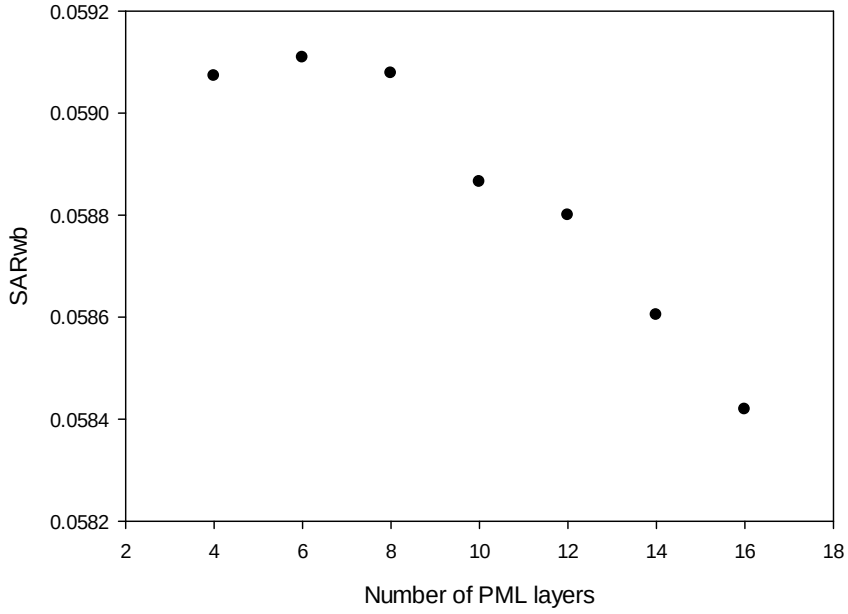

Figure 18: Influence of the number of PML layers on the final whole-body SAR results

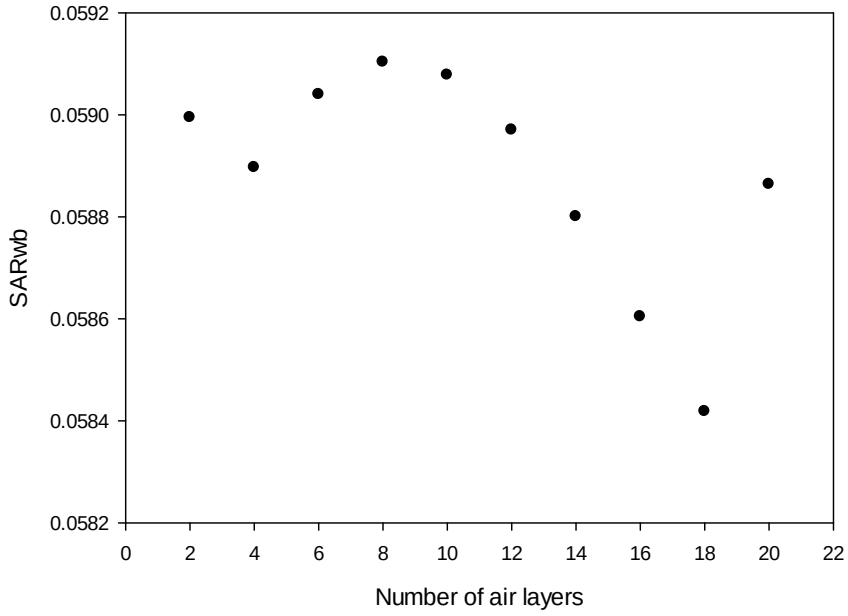

Figure 19: Influence of the number of air layers on the final whole-body SAR results

The results of varying the number of air and PML layers show, that these parameters have a minor effect on the results, as long as they are varied within reasonable limits. Figures 18 and 19 show, that the values of whole-body SAR change by less than 1.1 % in the whole range of tested cases.

The efficiency of clustering was evaluated and found to be very close to the theoretical limit of parallelization (Figure 20). The decrease of time following the ideal curve which would follow the equation $T_n=T_1/n$, where n is the number of computational nodes, T_1 is the time needed to solve the problem on a single node and T_n is the time needed to solve the problem on n nodes.

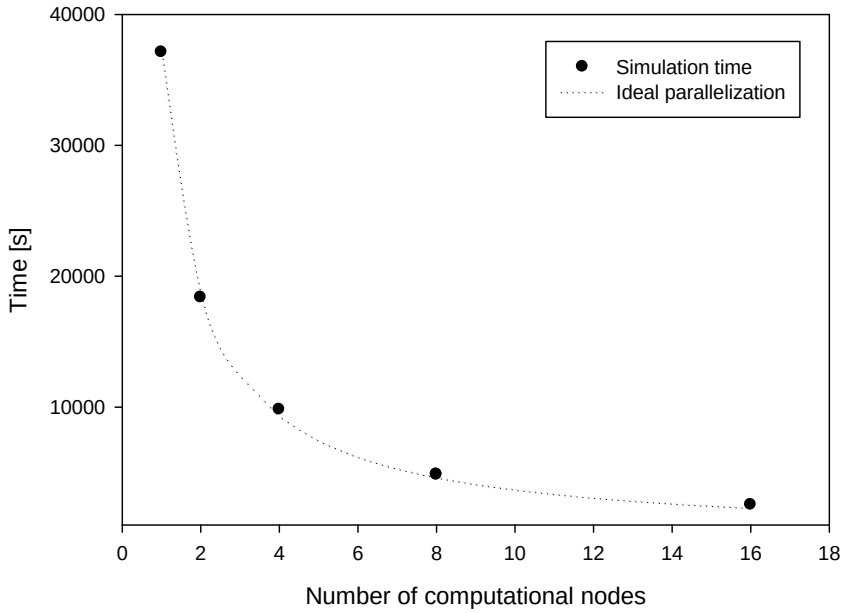

Figure 20: Time required for solving a model versus the number of computational nodes.

5. Comparison with third-party FDTD software SEMCAD X

The results of the two different code implementations were compared with the third party FDTD software package SEMCAD X, version 14.2.1 (SPEAG, Zurich, Switzerland). The values of whole-body SAR and tissue SAR were compared at two frequencies: 1.5 and 2 GHz (Table 5). The model used a 2mm voxel resolution and they all used the same incident field orientation. The model in the SEMCAD software is shown in Figure 21.

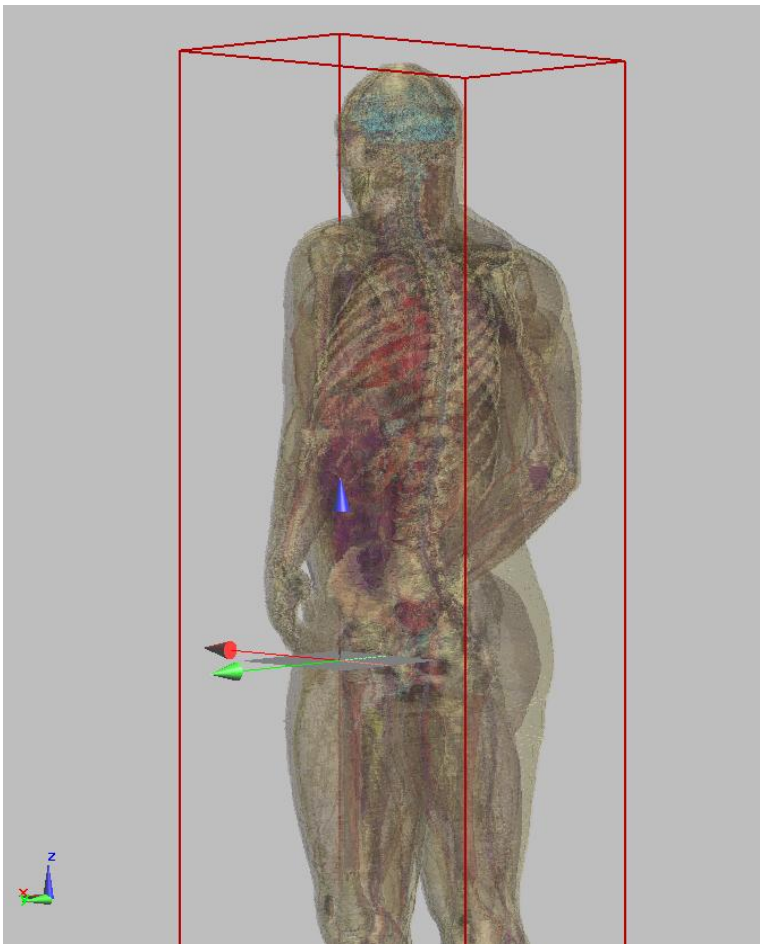

Figure 21: The orientation of the model in the coordinate system and the location of the planewave field source (red wire box).

At 1.5 GHz the results for whole body SAR were 0.049 W/kg, 0.058 W/kg and 0.60 W/kg in SEMCAD, C and Fortran codes, respectively. At 2 GHz these results were: 0.047 W/kg, 0.053 W/kg and 0.056 W/kg in SEMCAD, C and Fortran codes, respectively. This shows that the SEMCAD software package produces significantly lower results, but these may be due to differences in the SAR averaging and statistics implementations. Also the the SEMCAD software does not automatically ensure that a

steady state is reached in the model, as it doesn't compute SAR during the simulation, but only during post-processing.

The results of comparison of single tissues are consistent with the results for whole-body SAR in that the SEMCAD software produces values that are consistently lower than the two Brooks parallel FDTD codes.

	Tissue Mean SAR			
	1500 MHz		2000 MHz	
Tissue	SEMCAD	C	SEMCAD	C
Bile	0.069	0.086	0.030	0.037
Bladder	0.008	0.011	0.007	0.011
Blood	0.021	0.032	0.022	0.034
Blood_vessel	0.079	0.057	0.053	0.065
BodyFluid	0.084	0.066	0.044	0.049
Bone	0.019	0.028	0.022	0.029
Bone_cancellous	0.031	0.036	0.035	0.037
Brain_grey_matter	0.045	0.065	0.030	0.036
Brain_white_matter	0.029	0.047	0.018	0.025
Cartilage	0.092	0.110	0.086	0.094
Cerebellum	0.003	0.007	0.002	0.005
Cerebrospinal_fluid	0.044	0.065	0.028	0.037
Cornea	0.156	0.157	0.413	0.512
Eye_lens	0.069	0.132	0.208	0.227
Eye_sclera	0.159	0.143	0.223	0.239
Eye_vitreous_humor	0.219	0.207	0.303	0.335
Fat	0.024	0.021	0.015	0.021
GallBladder	0.050	0.041	0.020	0.025
Glands	0.077	0.087	0.083	0.088
Heart_muscle	0.012	0.016	0.004	0.010
Large_intestine	0.049	0.054	0.024	0.029
Liver	0.008	0.013	0.004	0.009
Lung	0.012	0.043	0.007	0.026
Lymph	0.033	0.032	0.018	0.022
Marrow_red	0.044	0.015	0.012	0.014
Mucosa	0.079	0.086	0.062	0.066
Muscle	0.051	0.064	0.043	0.052
Nails	0.070	0.119	0.107	0.237
Nerve	0.015	0.021	0.011	0.014
Pancreas	0.002	0.004	0.000	0.004
Skin	0.248	0.326	0.347	0.339
Small_intestine	0.033	0.038	0.016	0.022
Spleen	0.001	0.004	0.001	0.005
Stomach	0.032	0.035	0.013	0.020
Teeth	0.044	0.052	0.033	0.032
Tendon_Ligament	0.096	0.102	0.107	0.107
Testis	0.177	0.175	0.232	0.262
Total Selected	0.049	0.058	0.047	0.053

Table 5: Tissue maximum and mean SAR values in the SEMCAD and C code results

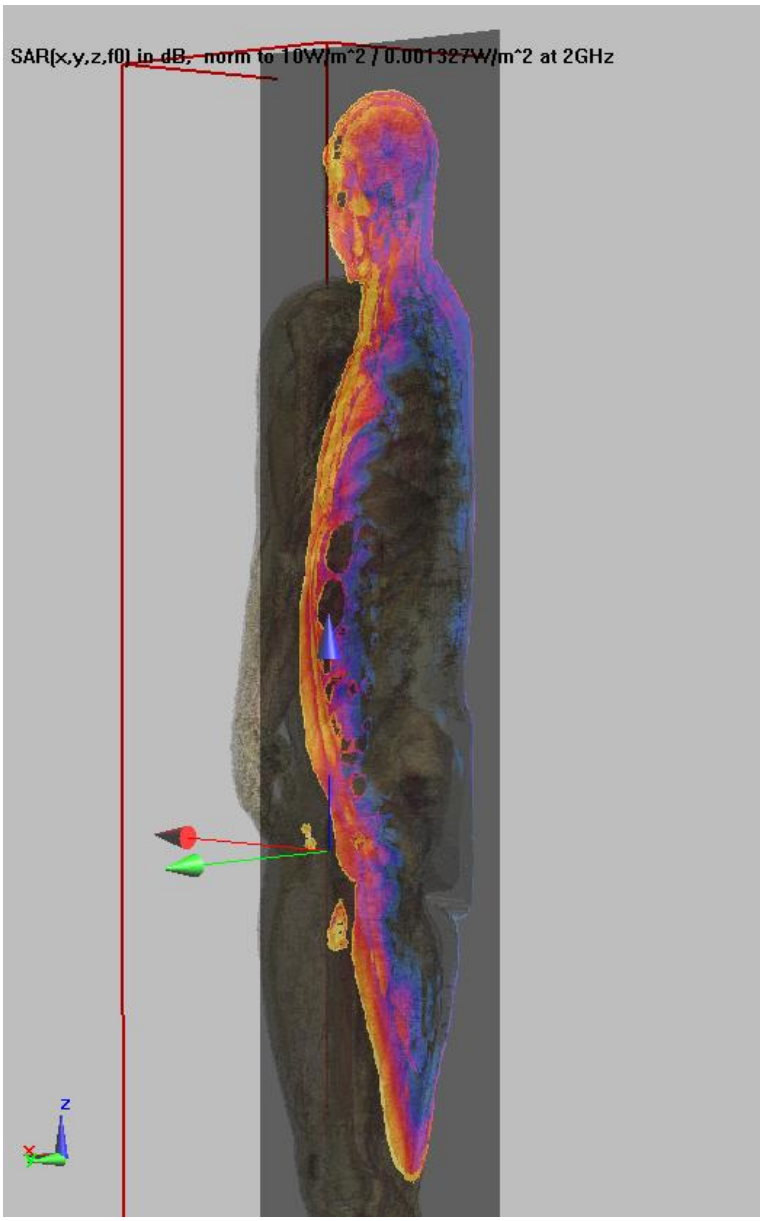

Figure 22: SAR in a vertical cross-section of the SEMCAD model.

The SAR values in Figure 22 were normalized to the same incident field power density (1mW/cm^2) as in the Brooks codes (Figure 16). A side-by-side comparison is made in Figure 23.

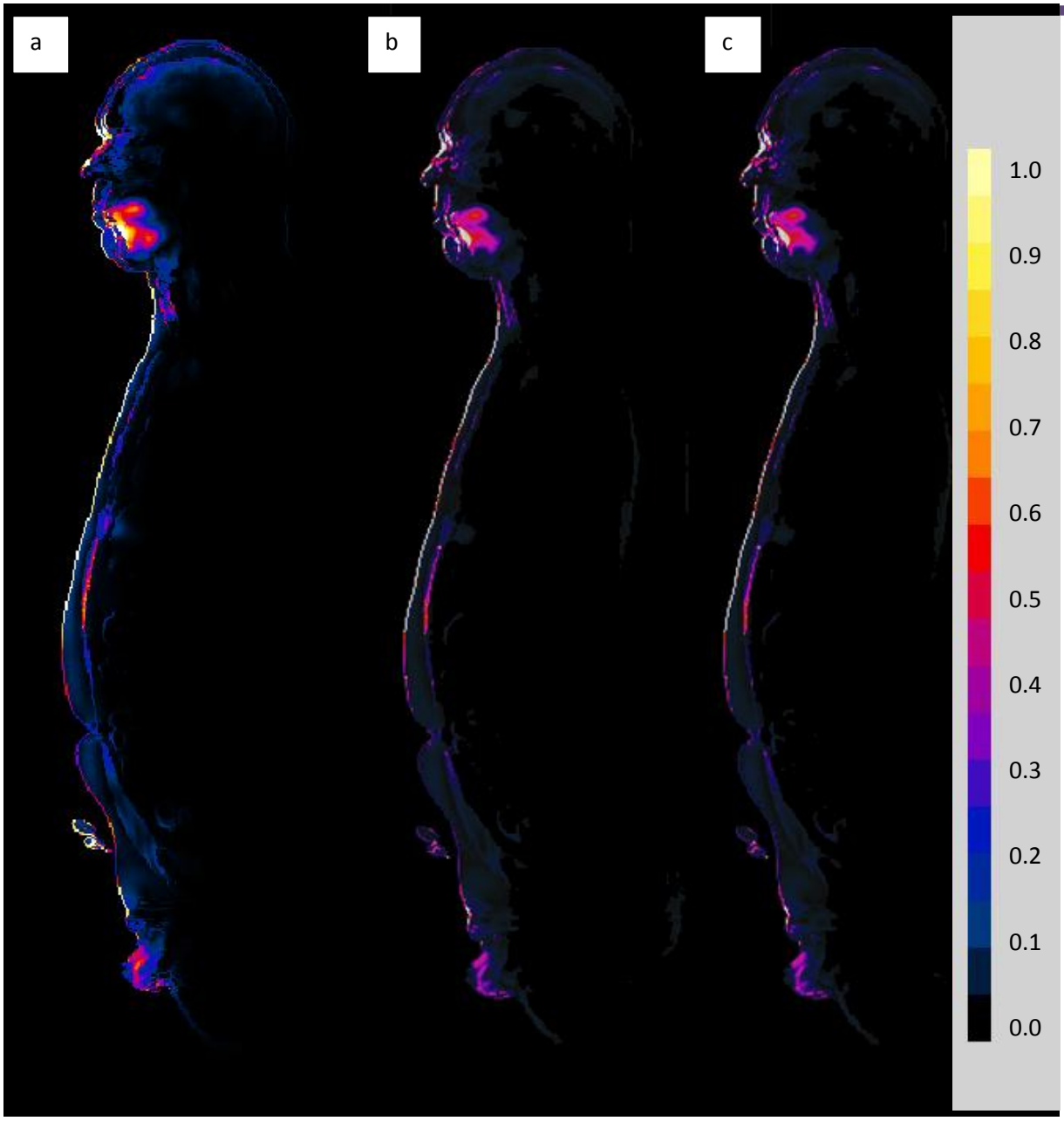

Figure 23: Slice showing the SAR distribution in the three different software packages. From left to right are a) SEMCAD, b) Fortran and c) C. All three plots use the same linear color-scale from 0 to 1 W/kg.

6. Rat model

A small rat model (51 by 22 by 114 voxels) was used as the final model in the comparison. The model was run at 5 different frequencies. The results are summarized in Table 6. Values of tissue SAR were also compared, and they agree best at frequencies from 300 to 500 MHz, with larger discrepancies appearing at 600 and 900 MHz. At frequencies from 300 to 500 MHz the largest differences in tissue mean SAR are +30 and -18 %, with the average difference being between -1 and 2 %. At 900 MHz, the differences increase to +444 and -85 % with the average difference between all tissues being 35 %.

Frequency [MHz]	Fortran [W/kg]	C [W/kg]	% difference
300	0.275907	0.281259	2%
400	0.4765121	0.475426	0%
500	0.7734072	0.78925	2%
600	0.8268738	0.90397	9%
900	0.5041003	0.594133	18%

Table 6: Values of whole-body SAR in the rat model

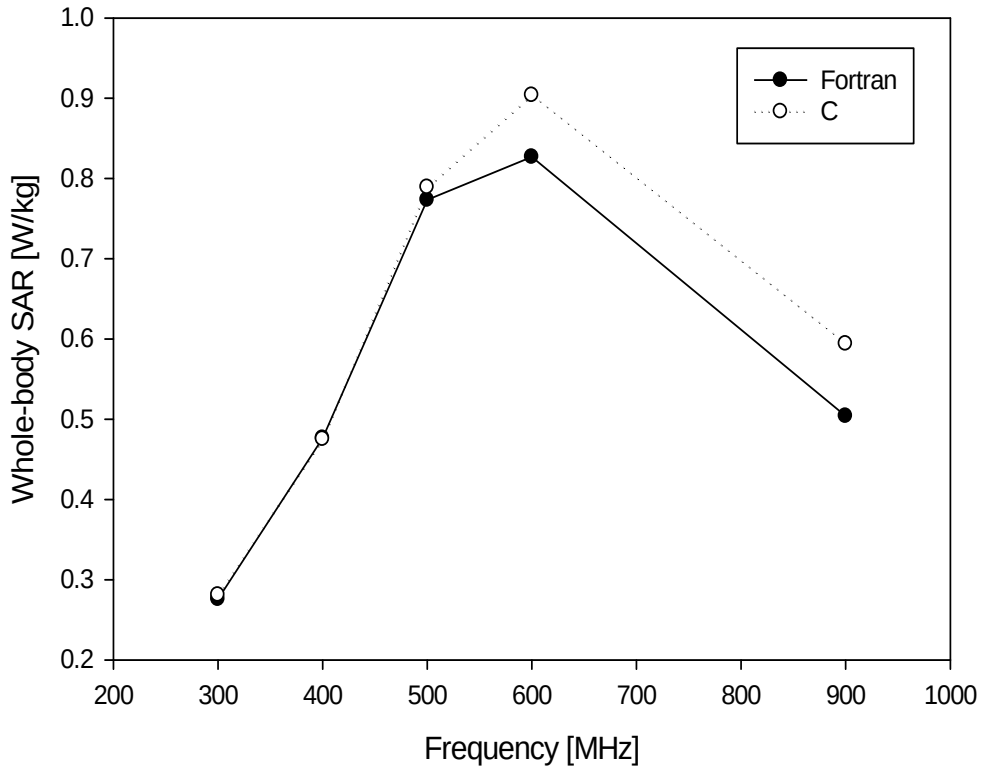

Figure 23: Whole-body SAR in the rat model versus frequency

7. Conclusion

The results show great consistency between the two different implementations of FDTD code across a wide variety of models and exposure scenarios. There are some minor outliers in the whole body SAR comparison, and some larger differences in the localized tissue SAR values. However, these can be explained by the fact that although the model and exposure details were the same, the criteria for finishing a simulation (i.e. the ratio between two successive whole-body SAR values) can be satisfied over the whole body, even if the distribution of power over the internal organs is not entirely stabilized yet.

The values would converge better if much longer simulations (in terms of number of halfcycles of the incident field, or number of time-steps of the Yee algorithm) were used. However, when tissue SAR values are much lower than the basic restrictions on localized SAR, the discrepancies in the range of 30 % are not significant. In fact, the best measurement setups for measuring localized SAR values in homogeneous liquid-filled phantoms have a measurement uncertainty around 1 dB (around 20 %), so differences in localized tissue values in this range actually represent a very good result.

The comparison with third party software SEMCAD also showed, that the results are very good and especially whole-body SAR values agreed very well, considering the differences in voxeling, normalization and most importantly SAR statistics algorithms.

Although some values show rather large differences, this could also be in part due to different hardware setups that the results were obtained on or due to different approaches to parallelization.

The conclusion is, that the two different implementations of the FDTD algorithm produce very similar results, to the point of being indistinguishable.

8. References

Gajšek, P., T.J. Walters, W.D. Hurt, J.M. Ziriax, D.A. Nelson, and P.A. Mason. 2002. Empirical validation of SAR values predicted by FDTD modeling. Bioelectromagnetics 23, no. 1: 37-48. doi:10.1002/bem.96.

Gajšek P, Hurt WD, Ziriax JM, Mason PA. Parametric dependence of SAR on permittivity values in a man model. IEEE trans. biomed. eng., Vol. 48, No. 10, pp 1169-1177, 2001

Gajšek, P., J.M. Ziriax, W.D. Hurt, T.J. Walters, and P.A. Mason. 2001. Predicted SAR in sprague-dawley rat as a function of permittivity values. Bioelectromagnetics 22, no. 6: 384-400. doi:10.1002/bem.66.

Gandhi OP, Numerical and experimental methods for dosimetry of RF radiation – some recent results, In Klauenberg BJ and Miklavčič D, (eds.) "Radio Frequency Radiation Dosimetry and Its Relationship to the Biological Effects of Electromagnetic Fields." Kluwer Academic Publishers B.V., Dordrecht, The Netherlands, 112-121, 2000

Hand, J W. 2008. Modelling the interaction of electromagnetic fields (10 MHz-10 GHz) with the human body: methods and applications. Physics in Medicine and Biology 53, no. 16 (August 21): R243-R286. doi:10.1088/0031-9155/53/16/R01.

Hurt WD (2000): Absorption characteristics and measurement concepts, In Klauenberg BJ and Miklavčič D, (eds.) "Radio Frequency Radiation Dosimetry and Its Relationship to the Biological Effects of Electromagnetic Fields." Kluwer Academic Publishers B.V., Dordrecht, The Netherlands, 39-52.

ICNIRP. 2009. Guidelines on limits of exposure to static magnetic fields. Health Physics 96, no. 4 (4): 504-514. doi:10.1097/01.HP.0000343164.27920.4a.

IEEE. 2006. IEEE Std C95.1 - 2005 IEEE Standard for Safety Levels with Respect to Human Exposure to Radio Frequency Electromagnetic Fields, 3 kHz to 300 GHz. IEEE Std C95.1-2005 (Revision of IEEE Std C95.1-1991).

Inman, MJ, and AZ Elsherbeni. 2005. Programming video cards for computational electromagnetics applications. IEEE Antennas and Propagation Magazine 47, no. 6 (December): 71-78.

Mason PA, Hurt WD, Walters TJ, D'Andrea JA, Gajšek P, Ryan KL, Nelson PA, and Ziriax JA (2000a): Effects of frequency, permittivity, and voxel size on predicted specific absorption rate values in biological tissue during electromagnetic field exposure, IEEE Microw. Theory & Techn, Vol.48, No 11, 2050-2057.

Mason, PA, TJ Walters, JW Fanton, DN Erwin, JH Gao, JW Roby, JL Kane, KA Lott, LE Lott, and RV

Blystone. 1995. Database created from magnetic-resonance images of a Sprague-Dawley rat, rhesus-monkey, and pygmy goat. FASEB JOURNAL 9, no. 5 (March): 434-440.

Talfove, Allen, and Susan C Hagness. 2005. Computational Electrodynamics: The Finite-Difference Time-Domain Method, Third Edition. Third edition. Norwood, MA: Artech House.

Yee, Kane. 1966. Numerical solution of initial boundary value problems involving maxwell's equations in isotropic media. IEEE Transactions on Antennas and Propagation 14, no. 3: 302-307.